LETTER

doi:10.1038/nature11310

Autistic-like behaviour and cerebellar dysfunction in Purkinje cell *Tsc1* mutant mice

Peter T. Tsai[1], Court Hull[2]*, YunXiang Chu[2]*, Emily Greene-Colozzi[1], Abbey R. Sadowski[1], Jarrett M. Leech[1], Jason Steinberg[1], Jacqueline N. Crawley[3], Wade G. Regehr[2] & Mustafa Sahin[1]

Autism spectrum disorders (ASDs) are highly prevalent neurodevelopmental disorders[1], but the underlying pathogenesis remains poorly understood. Recent studies have implicated the cerebellum in these disorders, with post-mortem studies in ASD patients showing cerebellar Purkinje cell (PC) loss[2,3], and isolated cerebellar injury has been associated with a higher incidence of ASDs[4]. However, the extent of cerebellar contribution to the pathogenesis of ASDs remains unclear. Tuberous sclerosis complex (TSC) is a genetic disorder with high rates of comorbid ASDs[5] that result from mutation of either *TSC1* or *TSC2*, whose protein products dimerize and negatively regulate mammalian target of rapamycin (mTOR) signalling. TSC is an intriguing model to investigate the cerebellar contribution to the underlying pathogenesis of ASDs, as recent studies in TSC patients demonstrate cerebellar pathology[6] and correlate cerebellar pathology with increased ASD symptomatology[7,8]. Functional imaging also shows that TSC patients with ASDs display hypermetabolism in deep cerebellar structures, compared to TSC patients without ASDs[9]. However, the roles of *Tsc1* and the sequelae of *Tsc1* dysfunction in the cerebellum have not been investigated so far. Here we show that both heterozygous and homozygous loss of *Tsc1* in mouse cerebellar PCs results in autistic-like behaviours, including abnormal social interaction, repetitive behaviour and vocalizations, in addition to decreased PC excitability. Treatment of mutant mice with the mTOR inhibitor, rapamycin, prevented the pathological and behavioural deficits. These findings demonstrate new roles for *Tsc1* in PC function and define a molecular basis for a cerebellar contribution to cognitive disorders such as autism.

To evaluate the role of *Tsc1* in cerebellar PCs, we generated mice with *Tsc1* deleted in cerebellar PCs ($L7^{Cre};Tsc1^{flox/+}$ (heterozygous) and $L7^{Cre};Tsc1^{flox/flox}$(mutant))[10]. Cre expression is high in PCs, and expression is evident by postnatal day 6 (P6)[11]. $Tsc1^{+/+}$ (wild-type), $L7^{Cre};Tsc1^{+/+}$ (L7Cre), $Tsc1^{flox/flox}$ (Flox), heterozygous and mutant mice did not show reduced survival, and weights were comparable across genotypes, unlike the severe phenotype of neuronal or glial *Tsc* mutants (Supplementary Fig. 1)[12].

To ensure that TSC1 function was impaired in PCs, we evaluated staining of phosphorylated S6 (pS6), a downstream effector of mTOR signalling. We expected TSC1 dysfunction to result in increased mTOR activity, and increased pS6 staining was detected in heterozygous and mutant PCs (Supplementary Figs 2–4). To assess the specificity of Cre-mediated recombination, we crossed $L7^{Cre}$ and *Rosa26* reporter mice and found only infrequent, scattered recombination in non-cerebellar areas, as described previously (Supplementary Fig. 5)[11]. We also examined pS6 staining in other brain regions but found no differences between mutants and controls, except in cerebellar PCs (Supplementary Fig. 6).

One of the most consistent pathologic findings in post-mortem studies of ASD patients is reduced cerebellar PC numbers[2]. In the mutant cerebellum, although basic cellular architecture was maintained in adult mice, the PC layer was abnormal with increased soma area and reduced PC numbers compared to control or heterozygous littermates (Fig. 1a, Supplementary Fig. 7). To investigate why PCs were decreased

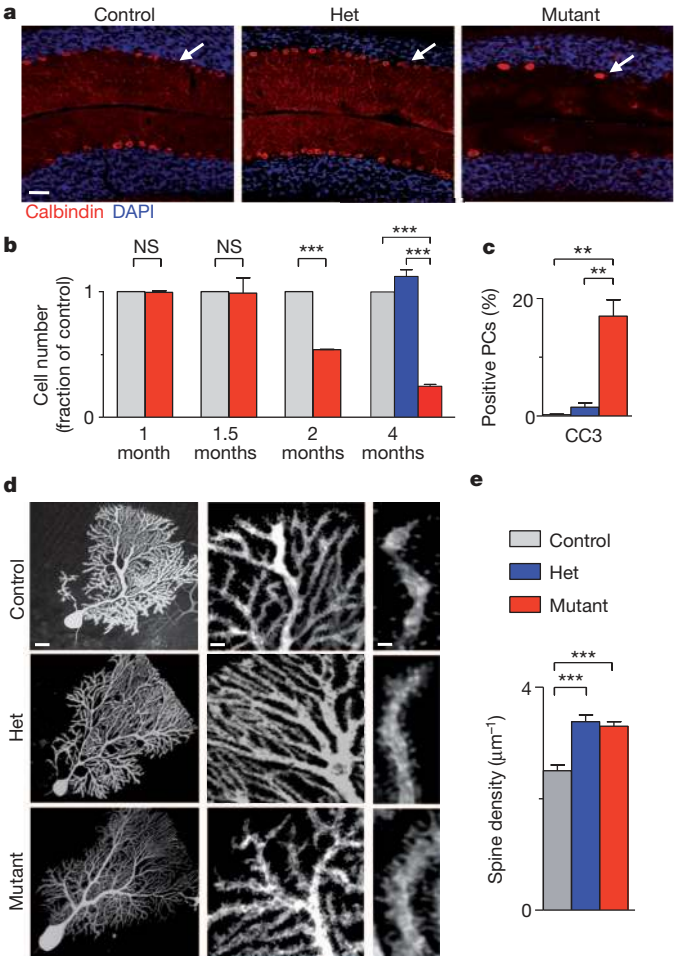

Figure 1 | PC *Tsc1* mutants display reduced PC numbers and abnormal PC morphology. **a**–**c**, Calbindin staining showed that mutants had reduced PC numbers (**a**; Het, heterozygote). Arrows, PCs. PC loss occurred by 2 months of age in mutants, but no PC loss was seen in heterozygotes at 4 months of age (**b**). NS, not significant. Increased cleaved caspase 3 (CC3) staining was found in mutants (**c**). In **b** and **c**, $n = 3$ mice for controls and mutants; $n = 2$ mice for heterozygotes; >500 cells per group. **d**, **e**, Mutant PCs displayed increased spine density ($n = 10$ cells, 3 mice for controls; $n = 10$ cells, 4 mice for heterozygotes; $n = 11$ cells, 3 mice for mutants). Middle and right panels, ×5 and ×20 magnifications of the left panel. ***$P < 0.001$, two-way analysis of variance (ANOVA), Bonferroni's post-hoc analysis. Scale bars in **a**.100μm; in **d**, 20 μm (left), 5 μm (middle) and 2 μm (right). Error bars, means ± s.e.m.

[1]The F.M. Kirby Neurobiology Center, Department of Neurology, Boston Children's Hospital, Harvard Medical School, Boston, Massachusetts 02115, USA. [2]Department of Neurobiology, Harvard Medical School, Boston, Massachusetts 02115, USA. [3]Laboratory of Behavioral Neuroscience, Intramural Research Program, National Institute of Mental Health, Bethesda, Maryland 20892, USA.
*These authors contributed equally to this work.

©2012 Macmillan Publishers Limited. All rights reserved

in mutants, we quantified PC numbers throughout development. Decreased cell numbers were first noted at 2 months of age, with a further reduction by 4 months of age, a reduction that was not seen in heterozygotes (Fig. 1b). As these findings suggested cell loss, we investigated markers of apoptosis and found increased TUNEL (TdT-mediated dUTP nick end labelling) and cleaved caspase 3 staining in mutant PCs at 7–8 weeks of age (Fig. 1c, and Supplementary Figs 8 and 9). Recently, neuronal stress in the cerebellum has been implicated in ASD pathogenesis[13], and studies have demonstrated critical roles for the TSC–mTOR pathway in mediating neuronal stress responses[14,15]. To investigate whether similar mechanisms were involved in *Tsc1*-mutant PC death, we evaluated markers for both endoplasmic reticulum (GRP78) and oxidative (haem oxygenase 1 (HO1)) stress and found significantly elevated levels of both markers (Supplementary Fig. 9).

As TSC–mTOR signalling has important roles in neuronal morphology and function[16,17], we also investigated whether *Tsc1* loss resulted in morphological changes in PCs at 4 weeks of age. TSC has known roles in the regulation of cell size[17,18], and the PC soma area was significantly increased in mutant, but not heterozygous, mice (Fig. 1d, Supplementary Fig. 10). TSC has also been implicated in regulating dendritic spine numbers[19], and we found increased spine density on heterozygous and mutant PC dendrites (Fig. 1d, e). Interestingly, decreased spine density has been reported in hippocampal and cortical neurons with *Tsc* loss[17,19,20], indicating that the mechanisms underlying the regulation of dendritic spines by TSC1 and TSC2 are diverse. We also found many axonal varicosities and abnormal axonal collaterals in mutants (Supplementary Fig. 11), consistent with known roles for TSC in regulating axonal morphology[16,21].

To investigate whether PC *Tsc1* mutants might show abnormal behaviours that are found in ASDs, we first evaluated social interaction, using a three-chambered assay of social approach and preference for social novelty. We found social impairments in both heterozygous and mutant animals, with no significant differences found between the time that they spent in the chamber or in interaction with the novel mouse versus the novel object (Fig. 2a). Subsequently, in a social novelty paradigm, control animals spent significantly more time in the chamber and in close interaction with the novel animal than with the familiar animal, whereas heterozygous and mutant animals displayed no significant preference for social novelty by either measure (Fig. 2b). We tested further whether mutants had impaired male–female social interactions and observed significant reductions in the time that the mutant mice spent interacting, compared with controls (Supplementary Fig. 12).

Taking into account the role of the cerebellum in motor functions, we investigated whether motor deficits contributed to social impairment. The motor activity of mutant mice was indistinguishable from littermates until approximately 7–8 weeks of age when mutants displayed initial signs of ataxia. Ataxia progressed, and by 4 months of age there were marked changes in gait parameters (Supplementary Fig. 13). However, heterozygotes displayed no ataxia (Supplementary Fig. 13), and locomotion during social testing and open-field testing was not significantly different between genotypes (Supplementary Figs 14 and15), indicating that motor impairments were not responsible for observed social deficits.

In rodents, social interaction depends largely on olfactory cues. We observed that comparable time was spent investigating three non-social olfactory cues—water, almond extract and banana extract (Supplementary Fig. 16)—indicating that olfactory function in mutants is intact. However, consistent with observed social impairment phenotypes, heterozygous and mutant mice demonstrated reduced investigation of social odours compared with controls, suggesting that impaired discrimination of social olfactory cues contributed to social deficits in mutants.

ASD patients also show repetitive behaviours and cognitive, behavioural inflexibility. To model the perseverative thinking and cognitive inflexibility exhibited by patients with ASDs, we tested animals in a reversal learning paradigm using a water T-maze. Two

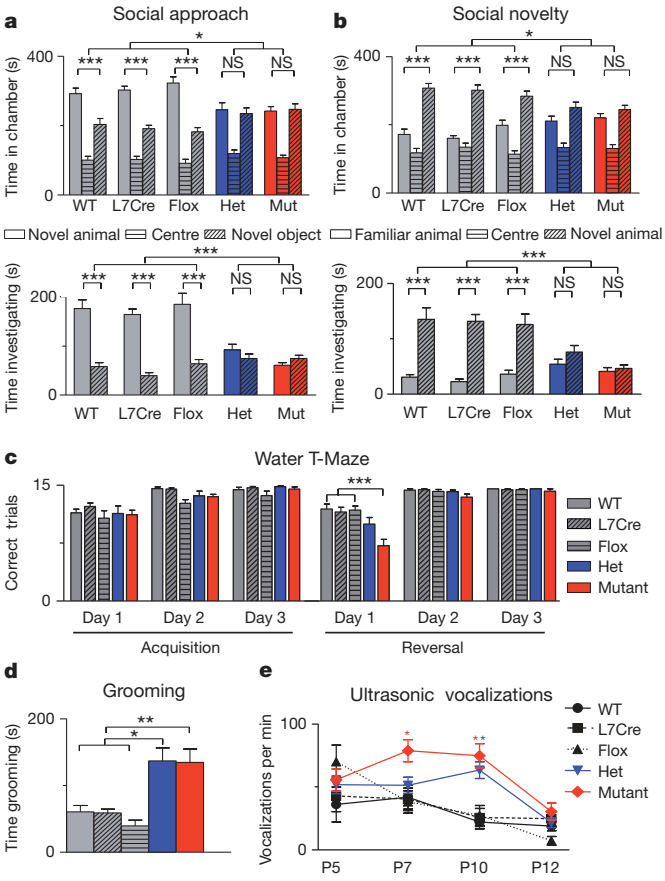

Figure 2 | PC *Tsc1* heterozygotes and mutants display autistic-like behaviours. **a**, In assays of social approach, unlike all control genotypes (WT, L7Cre and Flox), heterozygotes and mutants (Mut) showed no significant preference for a novel mouse over a novel object, as measured by time spent in a chamber (top panel) and time spent in close interaction with a novel mouse (bottom panel). **b**, Unlike controls, heterozygotes and mutants also failed to display preference for social novelty, as measured by time spent in the chamber (top panel) and in close interaction with either a familiar or a novel mouse (bottom panel) ($n \geq 11$ for each group). **c**, Mutants displayed normal acquisition of escape-platform location but impairments on day 1 of reversal learning in a water T-maze (total trials = 15; $n \geq 13$ for each group). **d**, Heterozygotes and mutants spent significantly more time self-grooming ($n \geq 11$ for each group). **e**, Heterozygote (P10) and mutant (P7 and P10) pups emitted significantly more ultrasonic vocalizations than controls ($n \geq 8$ for each time point and group). $^{*}P < 0.05$; $^{**}P < 0.01$; $^{***}P < 0.001$ (two-way ANOVA, Bonferroni's post-hoc analysis). Error bars, means ± s.e.m.

measures of learning performance were used—the number of correct trials and the number of trials needed before five consecutive correct trials were achieved—and showed that mutant animals had similar acquisition learning of a submerged escape-platform location (days 1–3) compared to control littermates (Fig. 2c and Supplementary Fig. 17). However, when the escape platform location was reversed, mutant animals demonstrated significantly impaired learning of the new platform location. We also examined repetitive behaviour in a repetitive grooming task and found significantly increased self-grooming rates in heterozygotes and mutants (Fig. 2d).

ASD-like behaviours also include deficits in communication. Murine pups use ultrasonic vocalizations to communicate with their mothers, and abnormal mother–pup communication has recently been shown in $Tsc2^{+/-}$ mice[22]. We evaluated ultrasonic vocalizations from P5–12 and, similar to reported ASD mouse models[23], we found increased vocalizations in both heterozygotes and mutants (Fig. 2e). Consistent with roles for *Tsc1* in regulating these early phenotypes, pS6 levels were elevated by P7 in mutant PCs (Supplementary Fig. 3). Motor deficits are also found in over 50% of patients with ASDs. To

©2012 Macmillan Publishers Limited. All rights reserved

evaluate whether mutants have impaired motor learning, we evaluated mutant animals before ataxia onset, using the accelerating rotarod test, and found significantly impaired motor learning in mutants (Supplementary Fig. 18).

The changes in PC morphology, combined with previous reports that *Tsc1* loss can alter synaptic properties[17,20], suggested that synaptic inputs to PCs might also be affected. PCs receive a single, strong climbing-fibre input and many weak granule-cell parallel-fibre inputs (Fig. 3a). However, we found no difference in the amplitude of single fibre climbing-fibre inputs between mutant and littermate controls at P28 (Fig. 3b). In control animals, when synapses are stimulated twice in rapid succession, climbing-fibre synapses depress, whereas parallel synapses facilitate, consistent with the high and low release probabilities of these synapses, respectively (Fig. 3b). The same characteristic plasticity was observed in mutants (Fig. 3b). We also stimulated parallel fibres, which produce both a direct excitatory short-latency parallel-fibre excitatory postsynaptic current (EPSC) and a disynaptic inhibitory postsynaptic current (IPSC) that arises from parallel-fibre activation of molecular layer interneurons (Fig. 3c). There was a trend towards a reduction in the ratio of the amplitudes of the EPSCs and IPSCs recorded in PCs, but this was not statistically significant (Fig. 3c). Although it is difficult to exclude a subtle effect on synaptic properties, these results indicate that in spite of morphological differences, significant alterations in synaptic transmission are not apparent in mutants.

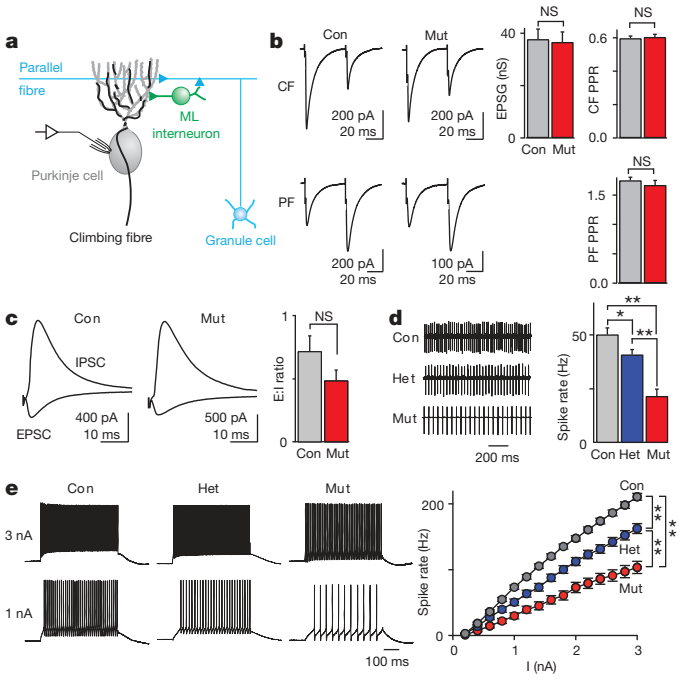

Figure 3 | PC excitability is reduced in PC *Tsc1* heterozygotes and mutants, but no significant difference is found in synaptic inputs to PCs. **a**, Schematic of the electrophysiological recording configuration and synaptic inputs onto cerebellar PCs. **b**, Electrical stimulation of climbing fibres (CF, top panel) and granule-cell-mediated parallel fibres (PF, bottom panel). Whole-cell voltage-clamp recordings showed no difference in the conductance (G) of single-fibre CF inputs ($n = 20$ cells, 5 mice for controls (Con); $n = 16$ cells, 5 mice for mutants; $P = 0.34$), or the paired-pulse ratio (PPR) of either CF or PF inputs (for CF PPR, $n = 8$ for controls, $n = 5$ for mutants; $P = 0.51$). EPSG, excitatory post synaptic conductance; ML, molecular layer. **c**, Electrical stimulation revealed no differences in the ratio of evoked synaptic excitation to inhibition (E:I ratio; $n = 29$ for controls, $n = 17$ for mutants; $P = 0.19$). **d**, Extracelluar recording of spontaneous PC spiking (left panel) revealed a significantly lower spike rate in heterozygotes and mutants (right panel; $n = 77$ cells, 12 mice for controls, $n = 62$ cells, 7 mice for heterozygotes, $n = 42$ cells, 9 mice for mutants). **e**, Whole-cell current-clamp recordings showed reduced excitability in PCs from heterozygotes and mutants compared to control PCs. Left, current injections of 1 and 3 nA produced fewer spikes in PCs from heterozygotes and mutants than in control PCs. Right, average data showed a reduced spike output for mutant PCs ($n = 77$ cells, 12 mice for controls, $n = 48$ cells, 7 mice for heterozygotes; $n = 43$ cells, 9 mice for mutants). $^*P < 0.05$; $^{**}P < 0.01$ (two-way ANOVA, Bonferroni's post-hoc analysis). Error bars, means ± s.e.m.

Previous studies of *Tsc1* have also focused on neurons that are quiescent in the absence of excitatory input, whereas PCs fire spontaneous action potentials even in the absence of synaptic inputs. Because PC firing rate is thought to be critical for encoding cerebellar output in deep cerebellar nuclei[24], we examined the intrinsic excitability of PCs using extracellular recordings, and found a significantly lower, graded spontaneous spiking rate in heterozygotes and mutants compared with controls (Fig. 3d). Moreover, current injection evoked fewer action potentials in heterozygous and mutant PCs, also in a graded fashion (Fig. 3e). A plot of firing frequency versus injected current shows that heterozygous and mutant PCs were significantly less excitable than controls (Fig. 3e). Injection of small hyperpolarizing currents resulted in smaller voltage changes in mutant and heterozygous PCs, indicating a decrease in the effective input resistance (Supplementary Fig. 19A), which has been described previously for hippocampal neurons[17]. This decrease in input resistance likely contributed to the reduced excitability of PCs in mutant and heterozygous animals. By 6 weeks of age there was an even more marked reduction in excitability in mutant mice (Supplementary Fig. 19B). Hence, despite receiving seemingly normal functioning synaptic inputs, the output of the cerebellar cortex of heterozygous and mutant animals seems to be strongly reduced, both tonically and in response to incoming excitatory drive. Our findings implicate reduced PC excitability as a potential mechanism underlying the abnormal behaviours in PC *Tsc1* mutant mice, consistent with clinical observations of impaired cerebellar function in ASD patients[9,25].

To evaluate whether the abnormal phenotypes seen in PC *Tsc1* mutant mice were modifiable as shown in other models of increased mTOR signalling[12,19,26], we treated animals with the mTOR inhibitor, rapamycin, starting at P7. Whereas vehicle treatment resulted in identical phenotypes to untreated cohorts, rapamycin treatment prevented the development of pathologic deficits in mutant animals, and mutant soma size and PC numbers were indistinguishable from controls (Fig. 4a and Supplementary Fig. 20).

We subsequently examined whether the abnormal behaviours could also be rescued with rapamycin treatment. In vehicle-treated mice, behavioural phenotypes were identical to untreated cohorts (Fig. 4b–c and Supplementary Figs 21–23); however, rapamycin treatment ameliorated the motor phenotypes seen in mutant animals in gait testing and the rotarod (Supplementary Figs 21 and 24). Rapamycin treatment also prevented deficits in the water T-Maze, with no significant differences seen between rapamycin-treated mutants and controls in both acquisition and reversal learning (Fig. 4b and Supplementary Fig. 22). In addition, following rapamycin treatment, mutants displayed social behaviour comparable to that of controls in both social approach and social novelty assays (Fig. 4c and Supplementary Fig. 23). Thus, rapamycin prevented both pathologic and behavioural phenotypes in *Tsc1* PC mutants, supporting the possibility of a therapeutic role for mTOR inhibition.

Our study shows that the TSC–mTOR pathway may have critical, novel roles in cerebellar PCs. We find that mice with homozygous and heterozygous loss of *Tsc1* in PCs demonstrated social impairment, restrictive behaviour and abnormal vocalizations; representative of the three core deficits in ASDs. Mutant mice, but not heterozygous mice, also displayed pathologic features found in ASD postmortem studies with reduced PC numbers and evidence of increased neuronal stress. Although PC loss has been reported in postmortem studies of ASD patients, several lines of evidence suggest that PC death cannot fully explain the abnormal behaviours seen in PC *Tsc1* mice. Prior to PC death, mutant mice displayed abnormal vocalizations and motor-learning impairments. In addition, mice with heterozygous loss of *Tsc1* showed no evidence of PC loss, but displayed autistic-like behaviours.

©2012 Macmillan Publishers Limited. All rights reserved

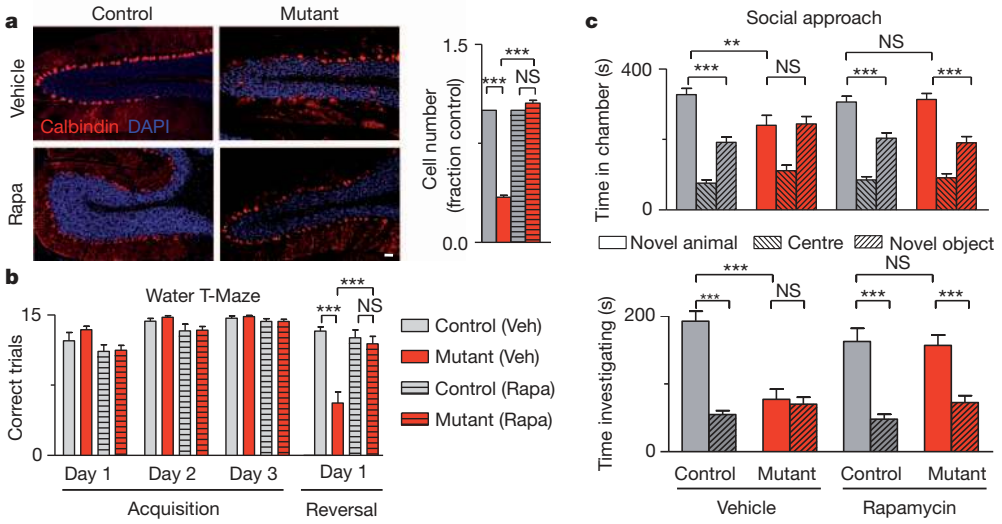

Figure 4 | Rapamycin treatment prevents pathological and behavioural abnormalities in PC *Tsc1* mutant mice. **a**, Treatment with rapamycin (Rapa) prevented cell loss seen in vehicle (Veh)-treated PC *Tsc1* mutants (left panel; scale bar, 100 μm), and quantification of cell numbers (right panel; $n > 500$ cells, 2 mice per group) **b**, **c**, Vehicle-treated mutants displayed behavioural deficits, whereas rapamycin-treated mutants displayed amelioration of these deficits, as shown using assays of reversal learning in the water T-maze ($n \geq 9$ in each group) (**b**) and social approach in the three-chambered apparatus ($n \geq 10$) (**c**). As behavioural phenotypes were not significantly different between the three control genotypes in untreated mice, control genotypes were pooled into a single group for these studies. $^{*}P < 0.05$; $^{***}P < 0.001$ (two-way ANOVA, Bonferroni's post-hoc analysis). Error bars, means ± s.e.m.

In this study, we also show that loss of *Tsc1* from cerebellar PCs is sufficient to result in abnormal autistic-like behaviours. These findings implicate the cerebellum in the neural circuitry mediating core features of autism. The cerebellum has been suggested previously to have roles in social interaction[27], and cerebellar abnormalities are associated with ASDs as well as cognitive and behavioural disturbances[28]. How the cerebellum modulates the abnormal behaviours of autism remains a topic of intense investigation. Autism has been proposed to be a disorder of abnormally distributed networks[29]. The cerebellum is connected, through the DCN, to these networks and cortical areas implicated in ASDs. Akin to its role in motor coordination, the cerebellum has been proposed to modulate these cognitive networks, with dysfunction resulting in abnormally regulated behaviours comparable to cognitive, behavioural dysmetria[30]. Our data displayed markedly impaired PC excitability in both heterozygotes and mutants. As PC firing rates are critical determinants of DCN output, by affecting DCN activity, PC dysfunction could alter these downstream neuronal networks, thereby contributing to abnormal autistic-like behaviours. Therefore, PC *Tsc1* mutants should provide a valuable experimental system to investigate the effects of PC dysfunction on these neuronal networks and other mechanisms contributing to the pathogenesis of ASDs.

METHODS SUMMARY

All behavioural procedures were reviewed and approved by the Animal Research Committee of Boston Children's Hospital. Descriptions of behavioural assays are provided in greater detail in the Methods. Experiments were performed with the examiner blind to genotype. Vehicle or rapamycin treatments (6 mg kg^{-1}) were given by intraperitoneal injection starting at P7 (a summary of the statistical analysis and the number of animals used in behavioural tests is provided in Supplementary Figs 25 and 26, and Supplementary Tables 1–3).

Full Methods and any associated references are available in the online version of the paper.

Received 22 August 2011; accepted 11 June 2012.
Published online 1 July 2012.

1. Prevalence. of autism spectrum disorders — Autism and Developmental Disabilities Monitoring Network, United States, 2006. *MMWR Surveill. Summ.* **58,** 1–20 (2009).
2. Bauman, M. L. & Kemper, T. L. Neuroanatomic observations of the brain in autism: a review and future directions. *Int. J. Dev. Neurosci.* **23,** 183–187 (2005).
3. Amaral, D. G., Schumann, C. M. & Nordahl, C. W. Neuroanatomy of autism. *Trends Neurosci.* **31,** 137–145 (2008).
4. Limperopoulos, C. *et al.* Does cerebellar injury in premature infants contribute to the high prevalence of long-term cognitive, learning, and behavioral disability in survivors? *Pediatrics* **120,** 584–593 (2007).
5. Jeste, S. S., Sahin, M., Bolton, P., Ploubidis, G. B. & Humphrey, A. Characterization of autism in young children with tuberous sclerosis complex. *J. Child Neurol.* **23,** 520–525 (2008).
6. Ertan, G., Arulrajah, S., Tekes, A., Jordan, L. & Huisman, T. A. Cerebellar abnormality in children and young adults with tuberous sclerosis complex: MR and diffusion weighted imaging findings. *J. Neuroradiol.* **37,** 231–238 (2010).
7. Weber, A. M., Egelhoff, J. C., McKellop, J. M. & Franz, D. N. Autism and the cerebellum: evidence from tuberous sclerosis. *J. Autism Dev. Disord.* **30,** 511–517 (2000).
8. Eluvathingal, T. J. *et al.* Cerebellar lesions in tuberous sclerosis complex: neurobehavioral and neuroimaging correlates. *J. Child Neurol.* **21,** 846–851 (2006).
9. Asano, E. *et al.* Autism in tuberous sclerosis complex is related to both cortical and subcortical dysfunction. *Neurology* **57,** 1269–1277 (2001).
10. Kwiatkowski, D. J. *et al.* A mouse model of TSC1 reveals sex-dependent lethality from liver hemangiomas, and up-regulation of p70S6 kinase activity in Tsc1 null cells. *Hum. Mol. Genet.* **11,** 525–534 (2002).
11. Barski, J. J., Dethleffsen, K. & Meyer, M. Cre recombinase expression in cerebellar Purkinje cells. *Genesis* **28,** 93–98 (2000).
12. Tsai, P. & Sahin, M. Mechanisms of neurocognitive dysfunction and therapeutic considerations in tuberous sclerosis complex. *Curr. Opin. Neurol.* **24,** 106–113 (2011).
13. Sajdel-Sulkowska, E. M., Xu, M. & Koibuchi, N. Increase in cerebellar neurotrophin-3 and oxidative stress markers in autism. *Cerebellum* **8,** 366–372 (2009).
14. Di Nardo, A. *et al.* Tuberous sclerosis complex activity is required to control neuronal stress responses in an mTOR-dependent manner. *J. Neurosci.* **29,** 5926–5937 (2009).
15. Reith, R. M., Way, S., McKenna, J. III, Haines, K. & Gambello, M. J. Loss of the tuberous sclerosis complex protein tuberin causes Purkinje cell degeneration. *Neurobiol. Dis.* **43,** 113–122 (2011).
16. Nie, D. *et al.* Tsc2-Rheb signaling regulates EphA-mediated axon guidance. *Nature Neurosci.* **13,** 163–172 (2010).
17. Tavazoie, S. F., Alvarez, V. A., Ridenour, D. A., Kwiatkowski, D. J. & Sabatini, B. L. Regulation of neuronal morphology and function by the tumor suppressors Tsc1 and Tsc2. *Nature Neurosci.* **8,** 1727–1734 (2005).
18. Meikle, L. *et al.* A mouse model of tuberous sclerosis: neuronal loss of Tsc1 causes dysplastic and ectopic neurons, reduced myelination, seizure activity, and limited survival. *J. Neurosci.* **27,** 5546–5558 (2007).
19. Meikle, L. *et al.* Response of a neuronal model of tuberous sclerosis to mammalian target of rapamycin (mTOR) inhibitors: effects on mTORC1 and Akt signaling lead to improved survival and function. *J. Neurosci.* **28,** 5422–5432 (2008).
20. Bateup, H. S., Takasaki, K. T., Saulnier, J. L., Denefrio, C. L. & Sabatini, B. L. Loss of Tsc1 *In vivo* impairs hippocampal mGluR-LTD and increases excitatory synaptic function. *J. Neurosci.* **31,** 8862–8869 (2011).

©2012 Macmillan Publishers Limited. All rights reserved

21. Choi, Y. J. *et al.* Tuberous sclerosis complex proteins control axon formation. *Genes Dev.* **22,** 2485–2495 (2008).
22. Young, D. M., Schenk, A. K., Yang, S. B., Jan, Y. N. & Jan, L. Y. Altered ultrasonic vocalizations in a tuberous sclerosis mouse model of autism. *Proc. Natl Acad. Sci. USA* **107,** 11074–11079 (2010).
23. Scattoni, M. L., Crawley, J. & Ricceri, L. Ultrasonic vocalizations: a tool for behavioural phenotyping of mouse models of neurodevelopmental disorders. *Neurosci. Biobehav. Rev.* **33,** 508–515 (2009).
24. De Zeeuw, C. I. *et al.* Spatiotemporal firing patterns in the cerebellum. *Nature Rev. Neurosci.* **12,** 327–344 (2011).
25. Ryu, Y. H. *et al.* Perfusion impairments in infantile autism on technetium-99m ethyl cysteinate dimer brain single-photon emission tomography: comparison with findings on magnetic resonance imaging. *Eur. J. Nucl. Med.* **26,** 253–259 (1999).
26. Zhou, J. *et al.* Pharmacological inhibition of mTORC1 suppresses anatomical, cellular, and behavioral abnormalities in neural-specific *Pten* knock-out mice. *J. Neurosci.* **29,** 1773–1783 (2009).
27. Insel, T. R. & Fernald, R. D. How the brain processes social information: searching for the social brain. *Annu. Rev. Neurosci.* **27,** 697–722 (2004).
28. Steinlin, M. Cerebellar disorders in childhood: cognitive problems. *Cerebellum* **7,** 607–610 (2008).
29. Müller, R. A. The study of autism as a distributed disorder. *Ment. Retard. Dev. Disabil. Res. Rev.* **13,** 85–95 (2007).
30. Schmahmann, J. D. Disorders of the cerebellum: ataxia, dysmetria of thought, and the cerebellar cognitive affective syndrome. *J. Neuropsychiatry Clin. Neurosci.* **16,** 367–378 (2004).

Supplementary Information is linked to the online version of the paper at www.nature.com/nature.

Acknowledgements We thank G. Corfas, M. Fagiolini, P. Rosenberg, S. Goldman and the Neurodevelopmental Behavioral Core of Boston Children's Hospital for assistance with behavioural experiments. We are grateful to C. Walsh, L. Benowitz and members of the Sahin laboratory for critical reading of the manuscript, and to M. Gregas for advice regarding statistical analysis. P.T.T. received support from the Developmental Neurology Training grant (T32 NS007473), American Academy of Neurology, and the Nancy Lurie Marks Family Foundation. This work and M.S. are supported in part by the National Institutes of Health (NIH; grant R01 NS58956), the John Merck Scholars Fund, Autism Speaks, the Nancy Lurie Marks Family Foundation, Boston Children's Hospital Translational Research Program, Manton Center for Orphan Disease Research and Boston Children's Hospital Intellectual and Developmental Disabilities Research Center (grant P30 HD18655). J.N.C. is supported by the Intramural Research Program, National Institute of Mental Health. W.G.R. is supported by the NIH (grant R01NS032405) and the Simons Foundation (grant SFARI 232304). Y.X.C. is supported by the Howard Hughes Medical Institute Medical Research Fellowship.

Author Contributions P.T.T. and M.S. conceived and designed the experimental approach, performed experiments and prepared the manuscript. C.H. and Y.X.C. designed and performed cerebellar slice experiments and assisted in manuscript preparation. E.G.-C., A.R.S. and J.M.L. assisted with behavioural experiments and statistical analysis. J.S. contributed to experimental quantification. J.N.C. provided training for behavioural phenotyping and contributed to behavioural experimental design and analysis. W.G.R. and M.S. supervised the project, and contributed to experimental design and analysis.

Author Information Reprints and permissions information is available at www.nature.com/reprints. Readers are welcome to comment on the online version of this article at www.nature.com/nature. The authors declare competing financial interests: details accompany the full-text HTML version of the paper at www.nature.com/nature. Correspondence and requests for materials should be addressed to M.S. (mustafa.sahin@childrens.harvard.edu) or P.T.T. (peter.tsai@childrens.harvard.edu).

©2012 Macmillan Publishers Limited. All rights reserved

METHODS

Mice. $L7^{cre};Tsc1^{flox/flox}$ (mutant) animals were generated by crossing *L7/Pcp2-Cre* ($L7^{Cre}$) transgenic mice[11] with floxed *Tsc1* mice ($Tsc1^{flox/flox}$)[10] to yield $L7^{Cre};Tsc1^{flox/+}$ progeny. These progeny were then crossed with one another or with $Tsc1^{flox/flox}$ animals to give litters consisting of control ($Tsc1^{+/+}$ (wild-type), $Tsc1^{flox/+}$, $L7^{Cre};Tsc1^{+/+}$ (L7Cre), or $Tsc1^{flox/flox}$ (Flox)) mice, heterozygous ($L7^{Cre};Tsc1^{flox/+}$) mice or mutant ($L7^{Cre};Tsc1^{flox/flox}$) mice. Only male animals were used for behavioural experiments except for analysis of ultrasonic vocalizations, in which both male and female pups were used. Mice were of mixed genetic backgrounds (C57Bl/6J, 129 SvJae and BALB/cJ). During analysis, germline deletion was discovered to occur in the mouse colony at a frequency of ~5% (more than 200 animals were tested). Genotyping for heterozygous mice would exclude these animals from this cohort, but it is possible that a small percentage of $L7^{Cre};Tsc1^{flox/-}$ mice were included in the mutant cohort. We therefore repeated behavioural analysis with a cohort of mutant ($L7^{Cre};Tsc1^{flox/flox}$) mice and littermate controls and found no significant differences with the previous mutant cohort (Supplementary Figs 25 and 26), and thus cohorts were combined for analysis. As behavioural data revealed comparable behavioural phenotypes between all untreated control ($Tsc1^{+/+}$, $Tsc1^{flox/flox}$ and $L7^{Cre};Tsc^{+/+}$) genotypes, these genotypes were pooled for behavioural studies involving rapamycin treatment. All experimental protocols were approved by the Animal Research Committee of the Children's Hospital, Boston.

Social interaction. Animals were tested for social interaction in the three-chambered apparatus (Dold Laboratories) as described previously[31]. Time spent in chambers and the number of crossings between chambers was recorded in an automated manner (National Instruments). Time spent interacting with the novel animal and object was recorded by an examiner with a stopwatch. Animals were tested between 7 and 9 weeks of age. For male–female interactions, tested males were placed into an open field with control females and evaluated for male-initiated interaction over a 5-minute period. All behavioural assays (including social interaction) were performed with the examiner blind to the genotypes.

Gait analysis. Animals were placed at the end of an apparatus that is 5 cm in width (preventing animals from turning around) and 56 cm in length, with paper placed along the floor of the entire apparatus. Apparatus walls consisted of opaque material and were 15 cm in height, preventing animals from looking over or escaping beyond walls. Paws were painted with red ink (forepaws) and black ink (hindpaws). The longest stride for each trial was taken as the stride length for that trial. Stride width was measured as the distance between the hind paws at time of the longest stride. Measurements were taken from 14–16-week-old animals.

Open field. Open-field testing was performed as described for a 15-min period[32]. Movement and time spent in centre quadrants were recorded by video camera and analysed by Noldus (Virginia) analysis software. Measurements were taken from animals aged 7–10 weeks.

Olfaction. Olfaction was tested as described previously[33]. Animals were presented sequentially with odours on cotton-tipped applicators: first, non-social odours, then social odours. Odours were presented in three consecutive trials per odorant stimulus (2 min per trial) in the following order: water, almond extract, banana extract, social odour 1, social odour 2. Social odours were swipes from cages containing unfamiliar gender- (male) and age-matched animals. Measurements were taken from animals aged 8–12 weeks.

Grooming. After habituation, animals were observed for 10 min, and time spent grooming was recorded as described[34]. Measurements were taken from animals aged 8–12 weeks.

Water T-Maze. Reversal learning was tested using the water T-maze as described[35]. On days 1–3, mice were given 15 trials and tasked to locate a submerged platform placed in one of the maze arms. After 15 trials on day 3, the platform was changed to the other maze arm. Mice were then tested for 15 additional trials (reversal day 1). Then for 2 subsequent days (reversal days 2 and 3), mice were given 15 trials per day. The number of correct trials and the number of trials required to achieve five consecutive correct trials were recorded. Measurements were taken from animals aged 8–12 weeks.

Ultrasonic vocalizations. Ultrasonic vocalizations were tested as described on postnatal days 5–12 (ref. 23). Pups were individually removed from their mother and placed inside a soundproof container in which three detectors were used to monitor vocalizations for 5 min. Calls were recorded using Ultravox recording software (Noldus)[36]. The maternal genotype in all experiments was $L7^{Cre};Tsc1^{flox/+}$.

Accelerating rotarod. Animals were tested using the accelerating rotarod, as described previously[37], over 5 consecutive days. Animals were tested before overt ataxia, between 5 and 7 weeks of age.

Slices. Acute sagittal slices (250–300-μm thick) were prepared from the cerebellar vermis of 4- and 6-week-old mutant and control littermates. Slices were cut in an ice-cold artificial cerebrospinal fluid (ACSF) solution consisting of (mM): 125 NaCl, 26 $NaHCO_3$, 1.25 NaH_2PO_4, 2.5 KCl, 1 $MgCl_2$, 2 $CaCl_2$ and 25 glucose (pH 7.3, osmolarity 310), equilibrated with 95% O_2 and 5% CO_2. Slices were initially incubated at 34 °C for 25 min, and then at room temperature before recording in the same ACSF.

Recordings. Visually guided (infrared DIC videomicroscopy and water-immersion ×40 objective) whole-cell recordings were obtained with patch pipettes (2–4 MΩ) pulled from borosilicate capillary glass (World Precision Instruments) with a Sutter P-97 horizontal puller. Electrophysiological recordings were performed at 31–33 °C.

IPSCs were recorded at the EPSC reversal potential, and parallel-fibre EPSCs were recorded at the IPSC-reversal potential. To measure climbing-fibre synaptic inputs, 500 nM NBQX (2,3-Dioxo-6-nitro-1,2,3,4-tetrahydrobenzo[f]quinoxaline-7-sulphonamide) was used to reduce the size of synaptic currents, and picrotoxin (20 μM) was used to block GABAergic inhibition. For experiments recorded at the EPSC-reversal potential and for climbing-fibre EPSCs, the internal pipette solution contained (in mM): 140 Cs-gluconate, 15 HEPES, 0.5 EGTA, 2 TEA-Cl, 2 MgATP, 0.3 NaGTP, 10 phosphocreatine-$Tris_2$, 2 QX 314-Cl. The pH was adjusted to 7.2 with CsOH. Membrane potentials were not corrected for the liquid junction potential. The EPSC and IPSC reversal potentials were determined in each experiment by adjusting the membrane potential until no EPSC or IPSC was evident; these potentials were approximately +15 mV for the EPSC reversal and −65 mV for the IPSC reversal. For current-clamp recordings, the internal solution contained (in mM): 150 K-gluconate, 3 KCl, 10 HEPES, 0.5 EGTA, 3 MgATP, 0.5 GTP, 5 phosphocreatine-$Tris_2$ and 5 phosphocreatine-Na_2. The pH was adjusted to 7.2 with NaOH. Current-clamp and extracellular recordings were performed in NBQX (5 μM), R-CPP (2.5 μM) and picrotoxin (20 μM) to block AMPA (α-amino-3-hydroxy-5-methyl-4-isoxazole propionic acid) receptors, NMDA (*N*-methyl-D-aspartate) receptors, and GABA subtype A ($GABA_A$) receptors, respectively. All drugs were purchased from Sigma-Aldrich or Tocris. Electrophysiolgical data were acquired as described previously[38].

Rapamycin treatment. Rapamycin was dissolved in 0.25% polyethylene glycol and 0.25% Tween before usage. Vehicle or rapamycin was administered intraperitoneally every Monday, Wednesday and Friday, with rapamycin dosed at 6 mg kg^{-1} per injection starting at P7. As behavioural data revealed comparable behavioural phenotypes between all untreated control ($Tsc1^{+/+}$, $Tsc1^{flox/flox}$ and $L7^{Cre};Tsc^{+/+}$) genotypes, these genotypes were pooled for behavioural studies involving rapamycin treatment.

Immunohistochemistry. Mice were perfused and post-fixed with 4% paraformaldehyde. Sections were prepared by cryostat sectioning and were stained with the following antibodies: PhosphoS6 (Cell Signaling), calbindin (Sigma, Cell Signaling), GRP78 (Stressgen), Haem Oxygenase-1 (Stressgen), cleaved caspase 3 (Cell Signaling). TUNEL staining was performed according to the manufacturer's instructions (Millipore).

Microscopy. Intracellular labelling of Purkinje cells was accomplished using recording pipettes filled with 0.05% biocytin (Tocris). Neurons in deeper portions of the Purkinje-cell layer were targeted and filled for 3 min, and then the pipette was slowly withdrawn so that the cell membrane could reseal. Slices (250-μm thick) were then fixed in 4% paraformaldehyde in 0.1 M phosphate buffer for 24 h, rinsed thoroughly in phosphate buffer solution (PBS) and incubated for 90 min in a PBS solution containing 0.5% Triton-X, 10% normal goat serum and streptavidin Alexa Fluor 488 conjugate (1:500, Life Technologies). Slices were then rinsed in PBS, mounted on Superfrost Plus slides (VWR International), air-dried, and coverslipped in Vectashield mounting media (Vector Labs). Immunohistochemical studies were captured using Zeiss Confocal LSM710. Images were processed and morphology quantified using ImageJ software with studies performed by examiner blinded to genotypes.

Statistics. Data are reported as mean ± s.e.m., and statistical analysis was carried out with GraphPad Prism software using one- and two-way ANOVA with Bonferroni's multiple comparison tests for post-hoc analysis unless otherwise specified.

31. Yang, M., Silverman, J. L. & Crawley, J. N. Automated three-chambered social approach task for mice. *Curr Protoc Neurosci* Ch 8, Unit 8 26 (2011).
32. Holmes, A. *et al.* Behavioral characterization of dopamine D5 receptor null mutant mice. *Behav. Neurosci.* **115,** 1129–1144 (2001).
33. Yang, M. & Crawley, J. N. Simple behavioral assessment of mouse olfaction. *Curr Protoc. Neurosci.* Ch 8, Unit 8 24 (2009).
34. Silverman, J. L. *et al.* Sociability and motor functions in *Shank1* mutant mice. *Brain Res.* **1380,** 120–137 (2011).
35. Bednar, I. *et al.* Selective nicotinic receptor consequences in APP_{SWE} transgenic mice. *Mol. Cell. Neurosci.* **20,** 354–365 (2002).
36. Kurejova, M. *et al.* An improved behavioural assay demonstrates that ultrasound vocalizations constitute a reliable indicator of chronic cancer pain and neuropathic pain. *Mol. Pain* **6,** 18 (2010).
37. Buitrago, M. M., Schulz, J. B., Dichgans, J. & Luft, A. R. Short and long-term motor skill learning in an accelerated rotarod training paradigm. *Neurobiol. Learn. Mem.* **81,** 211–216 (2004).
38. Hull, C. & Regehr, W. G. Identification of an inhibitory circuit that regulates cerebellar Golgi cell activity. *Neuron* **73,** 149–158 (2012).

©2012 Macmillan Publishers Limited. All rights reserved